Corrosion Science 148 (2019) 338–354

Contents lists available at ScienceDirect

Corrosion Science

journal homepage: www.elsevier.com/locate/corsci

Atmospheric corrosion of ZnAlMg coated steel during long term atmospheric weathering at different worldwide exposure sites

Dominique Thierry[a], Dan Persson[b,*], Gerald Luckeneder[c], Karl-Heinz Stellnberger[c]

[a] Institut de la Corrosion, 220 Rue Pierre Rivoalon, F-29200, Brest, France
[b] Swerea KIMAB, Isafjordsgatan 28A, 114 28, Stockholm, Sweden
[c] voestalpine Stahl GmbH, voestalpine Str. 3, 4020, Linz, Austria

ARTICLE INFO

Keywords:
A. Metal coatings
B. XRD
B. IR-spectroscopy
B. SEM-EDS
C. Atmospheric corrosion

ABSTRACT

The atmospheric corrosion of zinc aluminium magnesium (ZnAlMg) coated steel was studied in a worldwide exposure in Europe, East Asia and USA. The mass loss of ZnAlMg coated steel was about 2–3 times lower compared to hot dipped galvanised steel (HDG) after 4 years exposure. The corrosion of ZnAlMg coated steel was highly localised with selective corrosion attacks in the eutectic phases of the coating. Sulfate and chloride containing corrosion products were formed in the corrosion pits while zinc hydroxy carbonate and carbonate containing layered doubly hydroxides (LDH) formed mainly in the outer parts of corrosion attacks.

1. Introduction

Steel with coatings based on zinc are frequently used in the industry due their superior corrosion properties compared to carbon steel. For metal sheets, continuous hot dipped galvanized (HDG) steel and electro plated steel are the dominating products. While continuous hot dipped zinc coatings contain a small amount of Al to suppress the formation of the Zn-Fe phases during galvanizing, zinc coatings with even higher amounts of aluminium have been developed to further improve the corrosion resistance of the coatings. Zinc alloy coatings with both magnesium and aluminum have been commercially available since the late 1990s. The first developed coatings, such as Zn-11Al-3Mg-0.2Si (Super Dyma) and Zn-6Al-3Mg (ZAM), were relatively thick and primary used for aggressive corrosive conditions and building applications [1]. However, more recently, continuous hot dipped ZnAlMg have been introduced into the market. These coatings show improved corrosion properties compared to hot dipped galvanized steel and electro plated steel in salt spray and cyclic corrosion testing [2–7]

Despite the great technological importance of hot-dip galvanized steel most of investigations on atmospheric corrosion are performed on pure bulk metallic zinc while much less data exist on HDG and zinc alloyed coated steel. In a recent article the data on the atmospheric corrosion and the corrosion product formation on HDG from a worldwide exposure program were presented [8]. The corrosion attack on the zinc coating was localized for all exposure conditions. The composition and distribution of the corrosion products was related to the separation of the anodic and cathodic processes which causes variations of the local chemistry on the surfaces during the atmospheric corrosion process. Similar localised corrosion attacks have also been observed on bulk metallic zinc after exposures in marine atmospheres [9,10].

Although a significant body of work exist on the corrosion behaviour of ZnAlMg coatings during accelerated corrosion testing and in the laboratory, data on long term field performance of these new coating and a comparison with hot-dip galvanised steel are scarce. Diler et al. [11] reported that corrosion rate of ZnAlMg was about one half that of pure zinc panels after 6 months exposure in a marine atmosphere. An enhanced formation of sulfur containing corrosion products was seen on ZnAlMg coated steel compared to pure bulk zinc. This was attributed to quenching of the corrosion activity associated with the dissolution of Mg^{2+} and Al^{3+} from the coating. The corrosion behavior of ZnAlMg and HDG in different environmental conditions including marine, rural and urban locations was compared by Salgueiro et al [12] and a ratio of improvement between 2.4 and 3.3 of the corrosion rate was found after two years of exposure. A study of two different ZnAlMg alloy coatings in maritime environments for 3 years showed that the alloy coatings provided a similar improvement in corrosion resistance compared to HDG, but that ZnAlMg coatings were subjected to selective local corrosion attacks of the eutectic phases [13]. However, these

* Corresponding author.
E-mail address: dan.persson@swerea.se (D. Persson).

https://doi.org/10.1016/j.corsci.2018.12.033
Received 12 July 2018; Received in revised form 5 December 2018; Accepted 17 December 2018
Available online 26 December 2018
0010-938X/

Table 1
Nominal coating weight and steel thickness of the ZnAlMg coated steel and the HDG materials.

Metallic coating	Nominal coating mass, g/m^2	Steel thickness, mm
Hot dipped zinc	275	1.4
Zn-2%Mg-2%Al	200	0.9

studies were performed in European marine atmospheres and nothing is known on the performance of these coating in a worldwide situation.

The objective of the present study was to increase the knowledge about the corrosion behavior of ZnAlMg coated steel in different atmospheric environments. The composition of corrosion products and as well as the uniformity of the corrosion of ZnAlMg coated steel was studied in a wide range of climatic conditions at exposure sites in Europe, Asia and North America.

2. Experimental

2.1. Materials

A ZnAlMg coated steel with a nominal composition (Zn 2% Al 2% Mg) with a coating weight of 200 g / m^2 coating weight and Hot dipped galvanized steel was investigated, see Table 1. Details on the sample preparation prior to exposure can be find elsewhere [8].

The line hot dipped Zn % Al %Mg coating has a multiphase microstructure structure consisting of several phases. The coating is made up of primary Zn dendrites, a binary eutectic mixture consisting of Zn and the MgZn2 inter-metallic phase and ternary eutectic mixture (Zn, MgZn2, Al) [4,13].

2.2. Exposure conditions

The samples were oriented towards the sea, facing south and exposed at an inclination of 45° with respect to the horizontal for all exposure sites. The panels were installed on test racks with insulating fixings and precautions were made to avoid contamination between dissimilar coating materials. Table 2 lists all exposure sites together with their locations and basic characteristics of the exposures. A classification of the exposure sites was made in groups, depending upon the relative amount of chloride, SO_2 and NO_x and the distance to the sea. Mean values of chloride deposition and SO_2 concentration after 4 years

Table 3
Mean values of chloride deposition and SO_2 concentration after 4 years exposure.

Exposure site	Chloride deposition mg/m^2.day	SO_2 concentration µg/m^3
Brest (France)	1399	–
Wanning (China)	77	–
Daytona Beach (USA)	174	–
Sattathip (Thailand)	35	1
Bohus –Malmön Kattesand (Sweden)	321	0.7
Bohus –Malmön Kvarnvik (Sweden)	755	54*
Ijmuiden (The Netherlands)	–	6
Qingdao (China)	16	32
Singapore	18	25
Dubai	95	12
Cadiz (Spain)	26	1
Bangkok (Thailand)	–	1
Jiangjin (China)	–	218

* Very high value measured the first year of exposure not representative of this site.

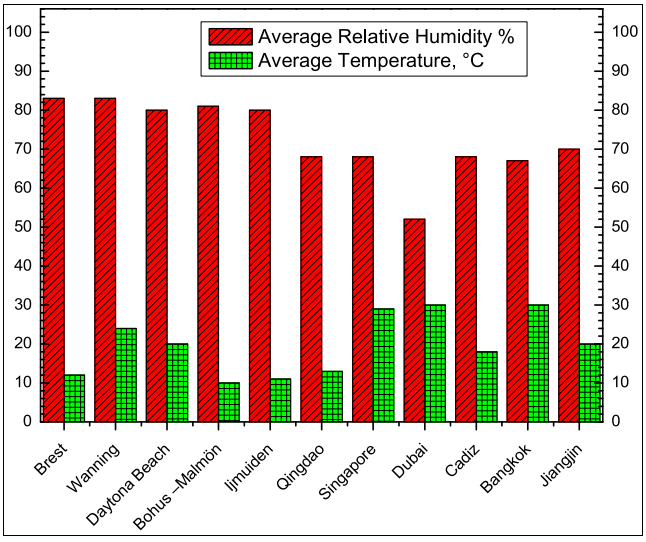

Fig. 1. Mean values of relative humidity (%) and temperature, °C on the exposure sites during 4 years exposure.

Table 2
Locations and characteristics of world-wide exposure sites.

Exposure site	Inclinination Orientation	Distance from sea	Longitude /Latitude.	Classification
Brest (France)	45 °S	< 5 m	4°33'W/48°21'N	Marine
Wanning (China)	45 °S	100 m	110°30'/18°58'N	Marine
Daytona Beach (USA)	45 °S	100 m	80°55'W/29° 5'N	Marine
Sattahip (Thailand)	45 °S	10 m	100°55'E/12°37'N	Marine
Bohus –Malmön Kattesand (Sweden)	45 °S	300 m	11°20' E/58°20'N	Marine
Bohus –Malmön Kvarnvik (Sweden)	45 °S	< 5 m	11°19' E/58°20'N	Marine
Ijmuiden (The Netherlands)	45 °S	2600 m	52°30'E/4°37'N	Marine/Industrial
Qingdao (China)	45 °S	10 m	120°44'E/36°05'N	Marine/Industrial
Singapore	45 °S	10 m	103°51'E/1°12'N	Marine/Urban
Dubai	45 °S	2000 m	55°02' E/24°58' N	Marine/Urban
Cadiz (Spain)	45 °S	750 m	6°12'W/36°32'"N	Marine/Urban
Ostrawa (Czech republic)	45 °S	~ 500 km	18°16'E/49°51'N	Industrial/Urban
Bangkok (Thailand)	45 °S	35 km	100°34'E/13°50'N	Industrial/Urban
Jiangjin (China)	45 °S	~ 900 km	106°15'E/29°19'N	Industrial/Urban

exposure are shown in Table 3. Mean values of the relative humidity and temperature for 4 years exposure are shown in Fig. 1.

The mass loss was determined on at least 3 replicates after 1, 2 and 4 years of exposure at the different sites (except at Sattahip where 3 years exposure was performed). The samples were brushed in order to remove non-adherent corrosion products, rinsed in flowing water and the corrosion products were removed by pickling according to ISO 8407:2009 standards. Pickling was done stepwise at the laboratory temperature using saturated glycine and the mass loss was evaluated from dissolution curves.

2.3. FT-IRRAS measurements

Analysis of the corrosion products were performed with Fourier transform infrared reflection absorption measurements (FT-IRRAS) using a Varian 7000 or a Bruker Vertex 70 spectrometer with Harrick's Seagull multi reflection accessory, using p-polarised light and an angle of incidence of 78 °C. The measurements were performed in the region 380–4000 cm^{-1}. An Au-mirror was used as background for the FTIR-measurements.

2.4. FTIR-imaging

FTIR imaging were made with a Bruker Vertex 70 spectrometer with a Hyperion 3000 microscope equipped with 64 × 64 focal plane array detector (FPA), The reflection measurements were performed using a 15x objective. The measurements were performed averaging 500 scan at a resolution of 8 cm^{-1} and making a ratio of the single beam spectra against a background spectra of a gold mirror.

2.5. SEM-EDS

The FEG-SEM equipment used in this work was a LEO 1530 with Gemini column, upgraded to a Zeiss Supra 55. The EDS detector was a 50 mm^2 X-Max Silicon Drift Detector (SDD) from Oxford Instruments. The cross sections of the samples analysed with SEM-EDS were prepared by mounting the samples in a two component epoxy resin and polishing the samples in ethanol.

2.6. GD-OES

Glow discharge optical emission spectroscopy (GDOES) was performed using a LECO GDS 850 A (LECO Technik GmbH). By means of calibration with reference materials (RM) and certified reference materials (CRM), the depth profiles are quantified to mass or atomic fractions vs. depth

2.7. X-ray diffraction

A Bruker AXS D8 Discover with a Cu-anode a SolX detector with energy window for Cu Kα was used for X-ray diffraction analysis Göbel mirror was used on the detector side. Measurements were performed at 5° angle of incidence.

3. Results

3.1. Mass loss of ZnAlMg coated steel and HDG

The ZnAlMg coated steel shows consistently lower mass loss compared to HDG after 1, 2 and 4 years exposure for all exposure sites, independently on the type of weathering conditions (e.g. marine, industrial and urban), as seen in Table 4. The calculated ratio between the mass losses of HDG vs ZnAlMg varies between 1.6–3.2 for samples exposed 4 years, with a mean value of 2.2 at all exposure sites. The ratio of mass loss for HDG and ZnAlMg after 1, 2 and 4 years exposure are shown in Fig. 2. The ratio is for many exposure sites higher for 1 and 2 years compared to 4 years exposure and varies between 2.1–4.9 (mean 3.4) and 1.7–4.2 8 (mean 3.1). This effect could be related to a combination of low mass losses for ZnAlMg during the first and second year of exposure at some sites and high initial corrosion rates for HDG. After 4 years exposure these variations decreases and the ratio of the mass losses is more similar for the different sites.

Table 4
Mass loss for HDG and ZnAlMg coated steel (coating weight 275 and 200 g/m^2 respectively) 1, 2 and 4 years exposure.

Mass loss g/m^2						
Exposure site	HDG 1 year	ZnAlMg 1 year	HDG[a] 2 years	ZnAlMg 2 years	HDG 4 years	ZnAlMg 4years[b]
Brest (M)	9.2	2.0	15.4	7.5	32.8	15.3(± 0.63)
Wanning (M)	19.9	7.1	33.3	10.3	51.4	27.0(± 1.02)
Daytona Beach (M)	11.5	2.5	28.6	6.7	31.0	13.9(± 1.8)
Sattahip(M)	6.4	1.3	10.8	1.8	13.6 (3 years)	5.5(± 1,02) (3 years)
Bohus –Malmön Kattesand	11.6	4.0	18.3	5.9	38.7	14.0(± 0.72)
Bohus –Malmön (M) Kvarnvik	18.2	7.2	36.6	8.6	55.4	26.1(± 0.52)
Ijmuiden (M/I)	7.3	2.2	11.8	6.8	24.4	12.3(± 0.86)
Qingdao (M/I)	9.5	4.6	25.2	11.3	41.3	18.8(± 1.18)
Singapore (M/U)	14.4	5.3	25.5	10.4	43.3	22.0(± 1.30)
Dubai(M/U)	15.1	3.4	24.5	10.3	47.3	21.8(± 0.36)
Cadiz(M/U)	4.3	1.8	6.5	2.8	12.8	7.8(± 0.9)
Ostrawa (I/U)	6.6	3.0	11.8	5.1	–	
Bangkok (I/U)	3.6	0.6	7.1	1.3	19.0	6.0(± 0.35)
Jiangjin (I/U)	8.9	4.2	16	9.7	28.3	16.3(± 0.46)

[a] Reference [8].
[b] including standard deviation.

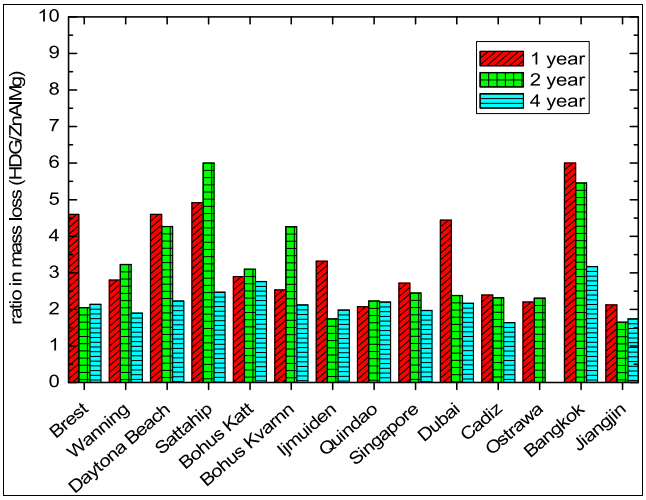

Fig. 2. Ratio between the mass loss for HDG and Zn2%Al2%Mg coated steel after 1, 2 and 4 years exposure.

However, it should be noticed that the observed ratio of the mass loss after 4 years of exposure is much lower than that measured after accelerated testing in neutral salt spray (about 12) or after cyclic corrosion testing (from 3 to 5) [14–16].

3.2. Investigations of corrosion product morphology and cross sections with SEM

The visual appearance of the surfaces of the ZnAlMg samples is consistently grey and dull for all exposure sites and exposure times. The amount of corrosion products on the surfaces is smaller compared to HDG which has white-grey corrosion products unevenly distributed on the surfaces at most test sites except for the pure industrial sites which have dark grey corrosion products. SEM investigations of exposed ZnAlMg coated samples showed that the corrosion products are unevenly distributed at the surfaces, but with the underlying microstructures of the substrate still visible on large parts of the surface. Figs. 3 and 4 show SEM micrographs of ZnAlMg coated steel after 6 and 24 months of exposure at the marine site of Brest and the industrial / urban site in Ostrawa. The corrosion products have an appearance of non-crystalline precipitates on the samples of the marine site while some small flake-like feature are found at some areas on the samples from Ostrawa.

The atmospheric corrosion ZnAlMg coated steel led to localised corrosion attacks which penetrate the metal coating down to the steel surface at some areas already after 6 months exposure. Cross sections of the ZnAlMg coating after exposure in the marine site of Brest and the industrial / urban site of Jiangjin after 2 years exposure are shown in Fig. 5. The corrosion attacks at these sites are preferably located to the eutectic phases of the alloy while the zinc rich phase remained unattacked,

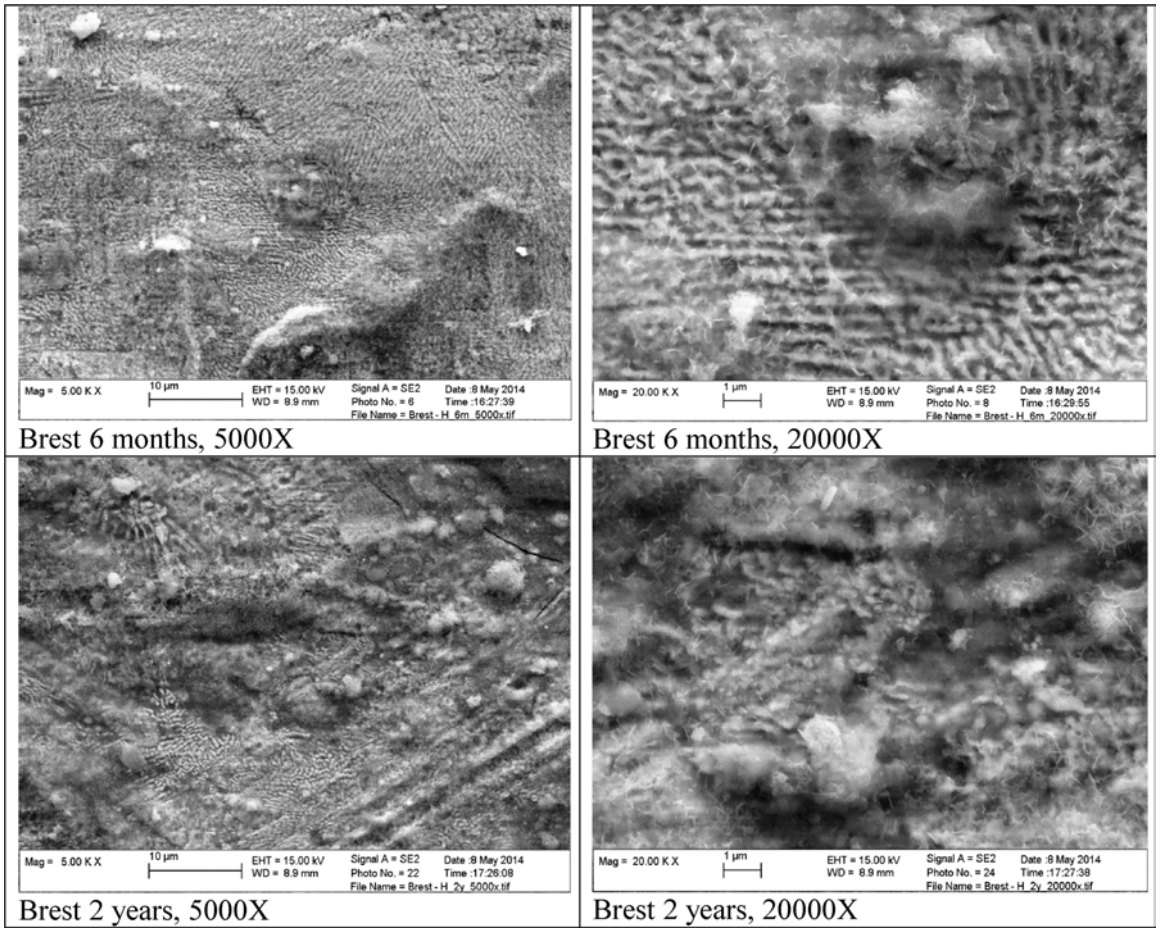

Fig. 3. SEM micrographs of Zn2%Al2%Mg coated steel samples exposed 6 months and 2 years in Brest.

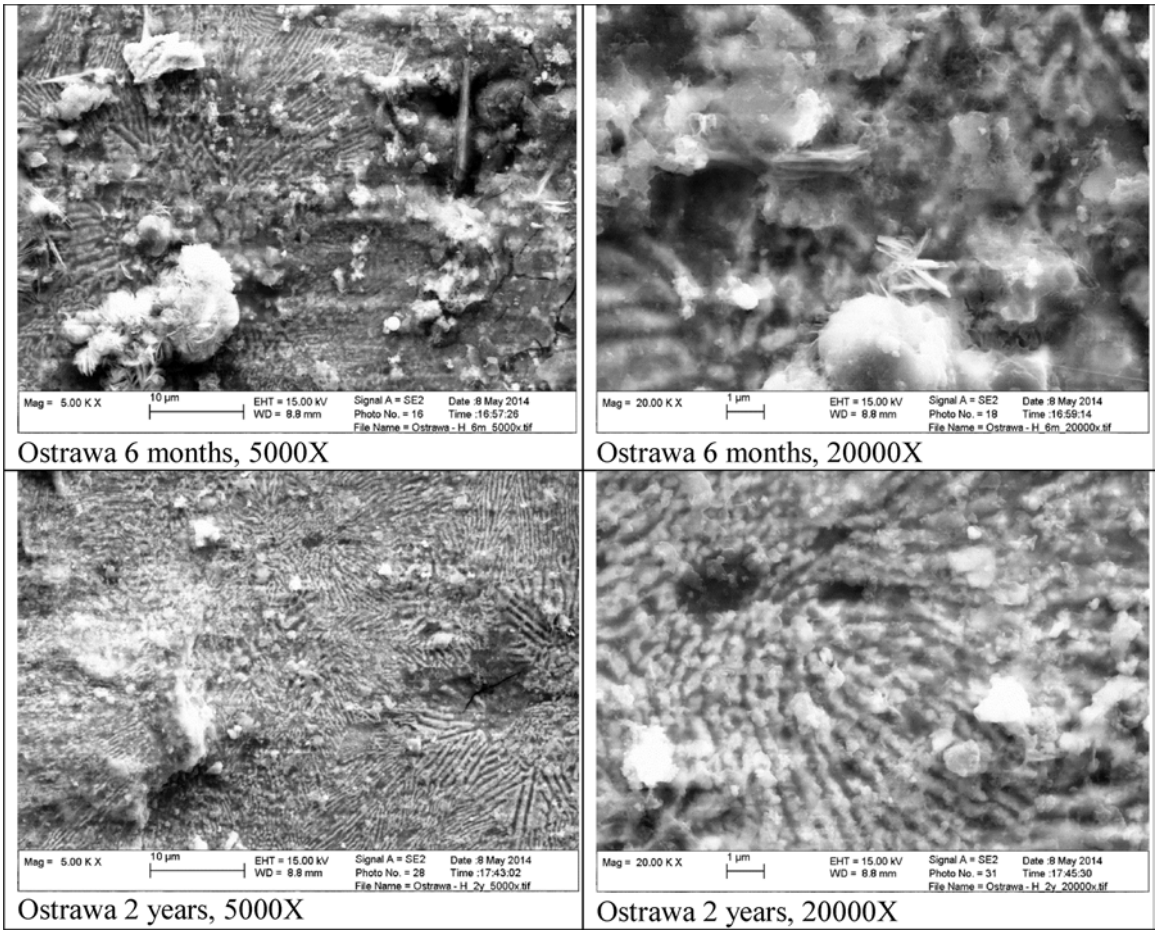

Fig. 4. SEM micrographs of Zn2%Al2%Mg coated steel samples exposed 6 months and 2 years in Ostrawa.

3.3. SEM-EDS analysis of cross section

SEM-EDS mapping and point analysis were performed on selected samples from all types of atmospheric conditions. EDS mapping of samples exposed at the marine site in Brest shows that S and Cl are enriched in the corrosion products where the eutectic areas have been attacked, see Figs. 6 and 7, for 6 months and 2 year exposure, respectively. In the corrosion pits the oxygen content increased as well as the aluminium content. On the other hand, the magnesium content was low in the corrosion pits. Thus, the results suggest that the corrosion products in the pits consist of an aluminium and zinc compounds containing sulphate and chloride.

For samples exposed in marine / industrial site as for instance Qingdao, the corrosion is also located mainly to eutectic phases with accumulation of sulphur and oxygen in the corrosion pits, see Fig. 8 The SEM-EDS results for the industrial / urban sites in Jiangjin are shown in Fig. 9. The corrosion attack is in the eutectic phases but the zinc rich phase is attacked to some extent as well. The O and S content is strongly enhanced in the corrosion product filled pit, but S and O are also present in the ternary eutectic phases close to the corrosion pit indicating an initial corrosion attack of the phase (Fig. 9).

Point analysis was performed on the cross sections of samples exposed 2 years in Brest and Jiangjin, see Figs. 10 and 11. The results show high Al content in the corrosion pit while the Mg content was very low. The wt% Zn in the corrosion pits is lowered compared to the phases in the coating. Sulphur is present in the pits at the marine site of Brest at a higher concentration than chloride and in the industrial / urban site of Jiangjin even higher contents of sulphur were detected.

3.4. FT-IRRAS and XRD analysis of the samples

FT-IRRAS measurements of the samples show mainly bands due to carbonate and sulphate containing corrosion products. The sulphate corrosion products have bands in the region from 950 to 1150 cm^{-1} due to the stretching vibrations of the sulphate ion, but overlapping bands due to hydroxyl groups can occur in lower wavenumber part of this region in the spectra as well. The strong stretching bands due to carbonate are found in the region from 1300-1600 cm^{-1}. The asymmetric stretching band due to carbonate ions in zinc hydroxy carbonate is split into two main bands located approximately at 1400 and 1500 cm^{-1}, which are further split in components separated 20–30 cm^{-1}. There are also other carbonate components which can contribute to the spectra, such as carbonate containing layered double hydroxides. These bands are more clearly visible in the spectra obtained by the FTIR-imaging measurements shown below. The spectra which contain larger contributions from sulphate have also bands from water

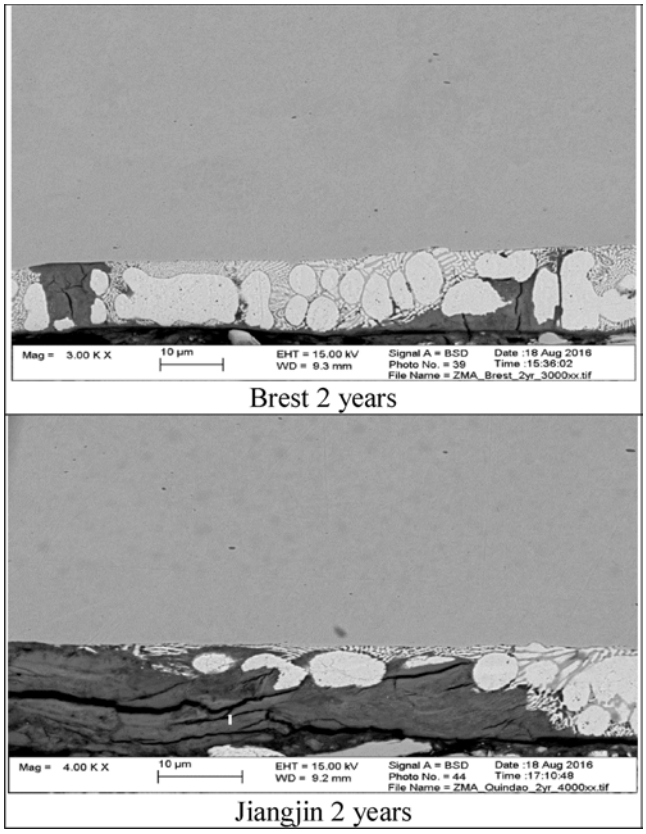

Fig. 5. SEM micrographs of cross sections of Zn2%Al2%Mg coated steel samples after 2 years exposure in Brest and Jiangjin.

molecules bonded in the corrosion products at 1600–1650 cm^{-1} and in the OH-stretch region at 3000–3600 cm^{-1}. Fig. 12 show FT-IRRAS spectra for HDG and ZnAlMg after 2 years of exposure in the marine test sites of Brest and Qingdao. As seen in the spectra the bands due to sulphate containing corrosion products are stronger for the ZnAlMg samples compared to HDG (Table 5).

The ratio of the sulphate to carbonate for the different exposure sites is higher for ZnAlMg compared to HDG for most exposure sites. The highest sulphate to carbonate ratio is observed for the industrial / urban sites and some of the marine / industrial sites while the lowest ratio is seen for the pure marine sites, see Fig. 13. The differences between the types of exposure sites according to the classification in Table 1 were similar for ZnAlMg and HDG.

The XRD analysis of the corrosion products indicates that the corrosion products for most samples contain zinc hydroxy sulphate and carbonate containing layered double hydroxides. There could also be contributions from chloride (and sulphate) containing LDH and / or zinc hydroxy chloride in the marine test sites, while sulphate containing LDH and aluminium hydroxy sulphate were present at all test sites. However, the peaks in XRD patterns of the corrosion products were generally broad and weak, indicating that the crystallinity of the corrosion products was low and the peaks can gave contributions from several overlapping peaks. XRD patterns for samples exposed in Brest and Ostrava for 2 years are shown in Fig. 14, and a summary of the suggested corrosion products from the XRD analysis is shown in Table 6.

3.5. FTIR imaging

FTIR-imaging of the exposed samples was used to visualize the distribution of the corrosion products on the exposed ZnAlMg coated steel surfaces. The analysis of the corrosion products by IRRAS, XRD and SEM-EDS suggest that carbonate and sulphate containing corrosion products are dominating, although chloride containing products are probably present at the marine exposure sites.

FTIR images based on the integrated areas of the carbonate and sulphate / hydroxyl bands for samples exposed at the marine site of Brest and industrial / urban site of Jiangjin are shown in Figs. 15 and 16 together with FTIR reflection spectra at selected points. The corrosion products at Brest are dominated by carbonates while sulphate containing species are the dominating products in Jiangjin. The carbonate bands are weak for this site. The high IR intensities of the carbonates in Brest are largely co-located to the same areas with the strongest sulphate bands. These are areas where the coating is attacked locally with the formation of sulphate and chloride containing corrosion products in the corrosion pits. The distribution of the corrosion products is consistent with the results from the SEM-EDS measurements on the cross sections in Figs. 7 and 9 which show localized attacks for the ZnAl Mg coating with the formation of sulphate and chloride containing corrosion products in the local corrosion attacks of the coating.

The spectra show that the composition of the carbonate corrosion product varies over the surface. As mentioned before, zinc hydroxy carbonate, $Zn_5(OH)_6(CO_3)_2$, has a carbonate asymmetric stretching band which is split in two main peaks located approximately at 1400 and 1500 cm^{-1}. These peaks are further split in components separated 20–30 cm^{-1}. The XRD and FT-IRRAS indicate further the formation of a carbonate containing layered double hydroxide (such as, $Zn_2Al(OH)_6(CO_3)_{1/2}{\cdot}H_2O$), which have single asymmetric carbonate stretching band around 1340–1370 cm^{-1} [17]. This is confirmed by the FTIR imaging measurements which shows that spectra obtained at different areas have different contributions from carbonates corresponding to zinc hydroxy carbonate and layered double hydroxide, as seen in the spectrum in Fig. 17. For samples exposed in Qingdao the layered double hydroxide is the dominating carbonate compound on the surface as inferred from the single carbonate asymmetric band. Sulphate / hydroxyl bands are present on a large part of the surface with stronger intensities in areas where the corrosion attacks have penetrated the ZnAlMg coating.

3.6. GD-OES analysis

GD-OES was used to obtain information about changes in the content C and S of the coated samples after exposure. The corrosion product analysis showed that carbonate and sulphate containing corrosion products are the dominating corrosion products on the samples after exposure, and with some chloride containing corrosion products on the marine test sites. The ratio of the coating weights for Sulphur and Carbon after exposure was determined from the GD-OES data for the outermost part of the coating and for the whole coating thickness for ZnAlMg and HDG after exposure at selected sites. The ratio of the Sulphur to Carbon content is lowest for HDG exposed at the marine test site in Brest while it is higher for the ZnAlMg material at the same exposure site. Highest S/C ratios are observed for the marine / industrial site in Qingdao and the industrial /urban site in Jiangjin. This is consistent with the FTIR results which show the same trends for the sulfate to carbonate ratios, see Fig. 13.

The GD-OES results indicate also that the S to C ratio is lower in the

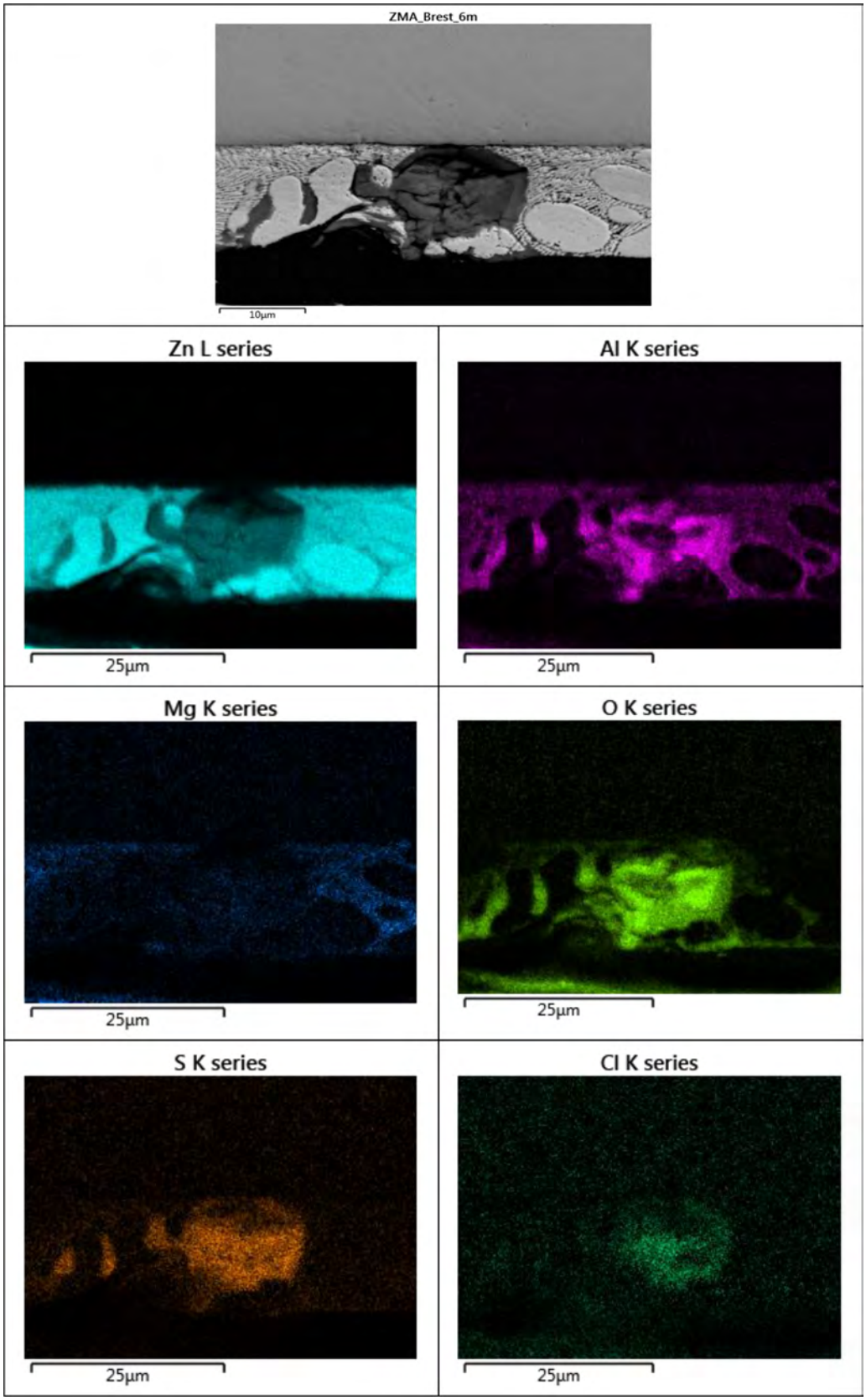

Fig. 6. SEM-EDS maps of Zn, Al, Mg, O, S and Cl for a cross section of Zn2%Al2%Mg coated steel exposed 6 months in Brest.

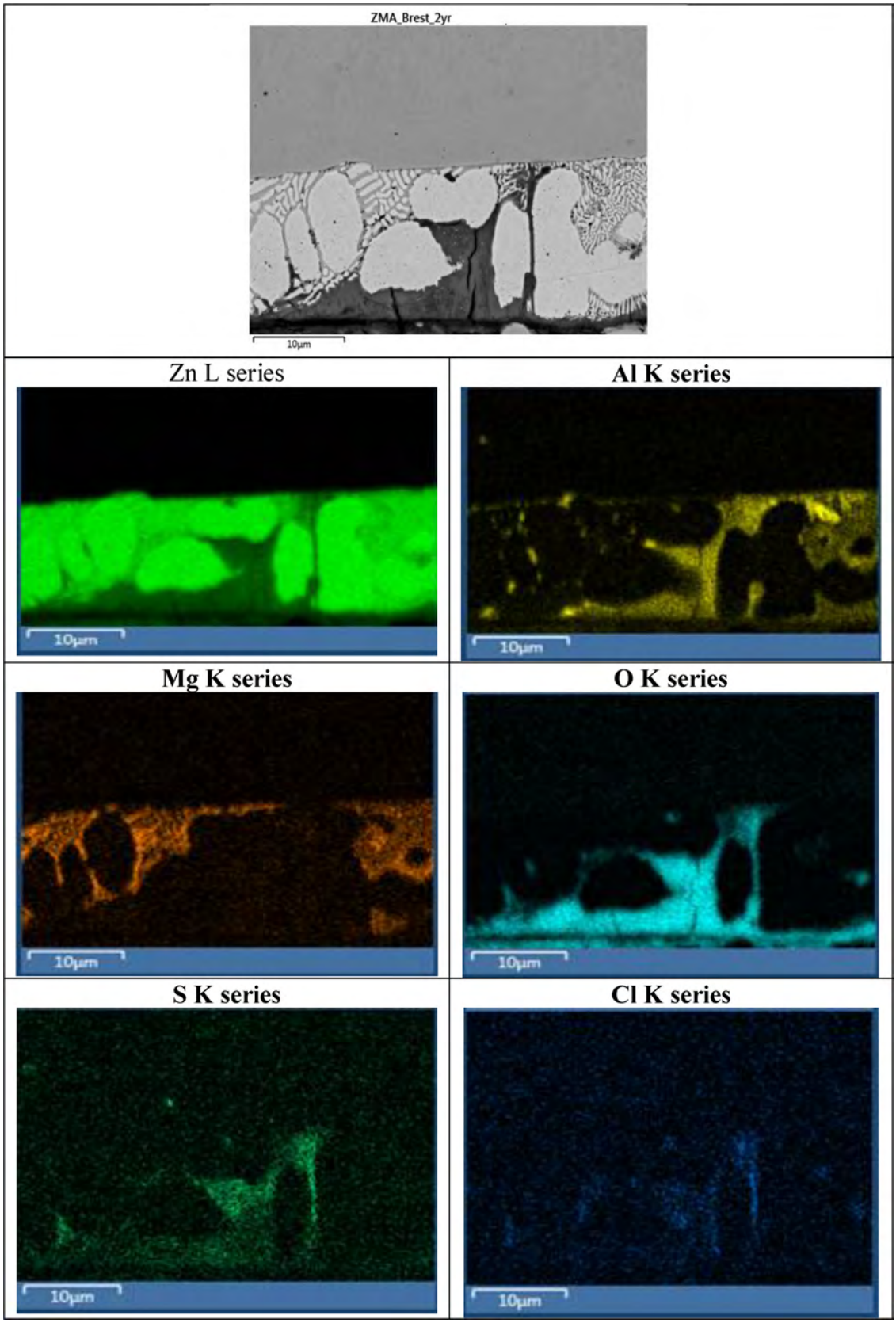

Fig. 7. SEM-EDS maps of Zn, Al, Mg, O, S and Cl for a cross section of Zn2%Al2%Mg coated steel exposed 2 years in Brest.

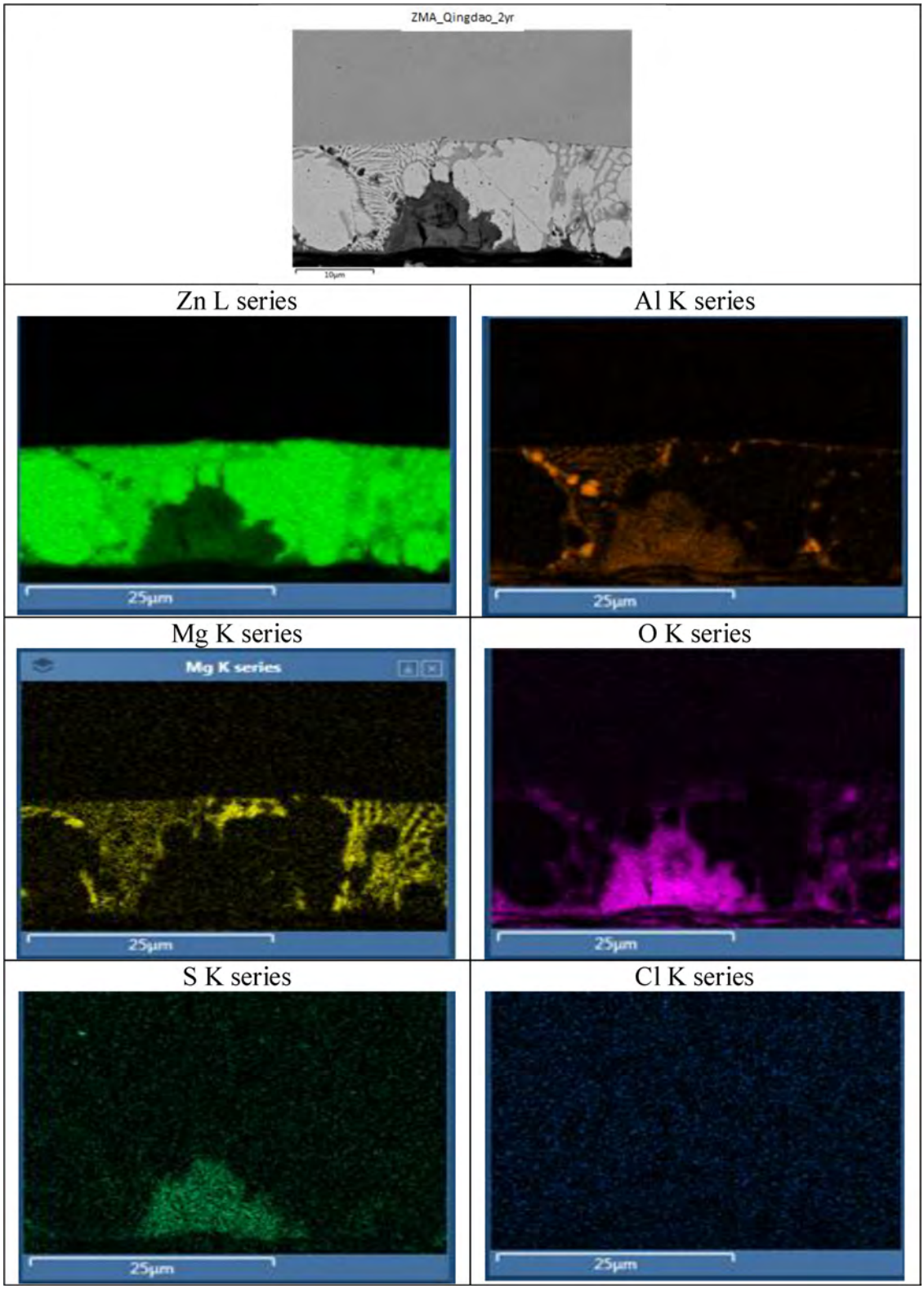

Fig. 8. SEM-EDS maps of Zn, Al, Mg, O, S and Cl for a cross section of Zn2%Al2%Mg coated steel exposed 2 years in Qingdao.

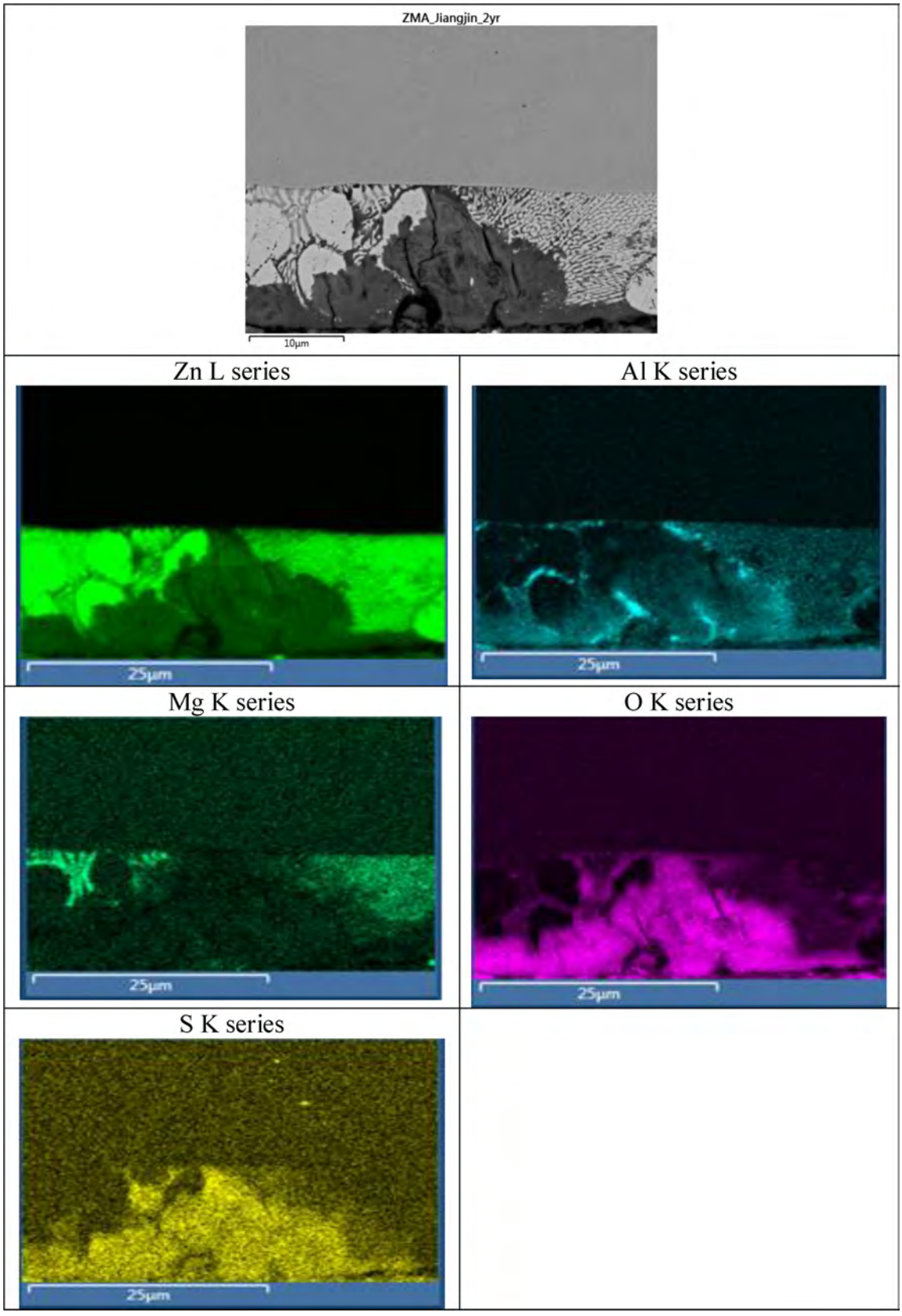

Fig. 9. SEM-EDS maps of Zn, Al, Mg, O, S and Cl for a cross section of Zn2%Al2%Mg coated steel exposed 2 years in Jiangjin.

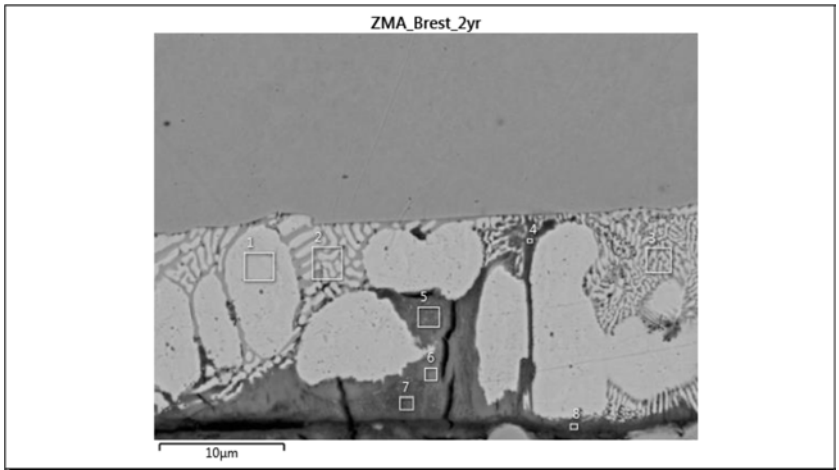

Element (Wt%)	1	2	3	4	5	6	7	8
O	0.55	1.03	0.45	6.60	12.23	15.15	14.63	8.30
Mg		5.24	3.38	0.55	0.38	0.46	0.42	0.47
Al	0.69	0.75	4.67	9.52	3.55	9.30	10.19	2.56
S				1.55	1.62	1.03	1.43	0.61
Cl				1.27	0.81	0.49	0.60	0.30
Zn	91.40	85.30	83.72	68.84	69.67	63.09	61.97	75.77

Fig. 10. SEM-EDS point analysis of cross sections of Zn2%Al2%Mg coated steel exposed 2 years in Brest.

outer parts of the exposed coatings. This can be explained by the formation of carbonate containing corrosion products in the outer parts of the coating while sulphate based corrosion products are formed preferably in the corrosion pits which penetrates the coating towards the steel surface. However, it is assumed that the sputtering rate is similar for the corroded parts of the coating and the metallic parts, which may be not fully justified. The carbon signal will also have contributions from carbon contamination, and not only from carbonate (Table 7).

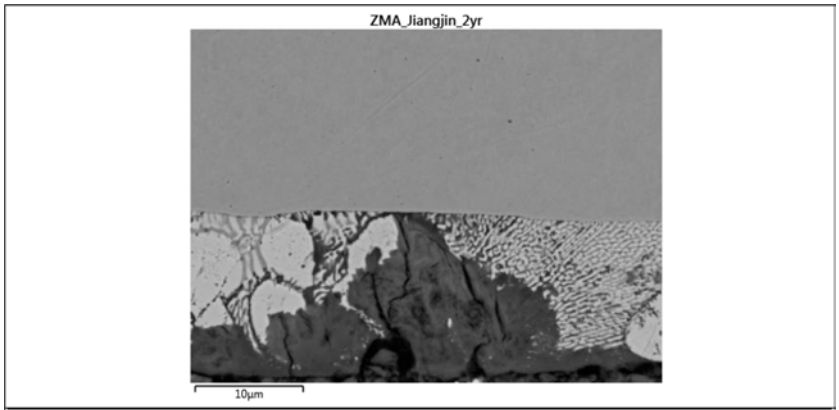

Element (Wt%)	1	2	3	4	5	6	7	8	9
O	0.74	2.92	2.35	11.06	15.33	21.39	25.27	25.41	21.15
Mg		4.66	3.56		0.13	0.25	0.19	0.36	
Al	0.66	0.58	3.13	5.54	4.18	6.21	7.19	7.59	10.11
S				3.39	2.88	3.31	3.11	3.18	3.18
Zn	91.89	80.72	81.44	67.19	64.30	54.81	50.59	44.83	53.07

Fig. 11. SEM-EDS point analysis of cross sections of Zn2%Al2%Mg coated steel exposed 2 years in Jiangjin.

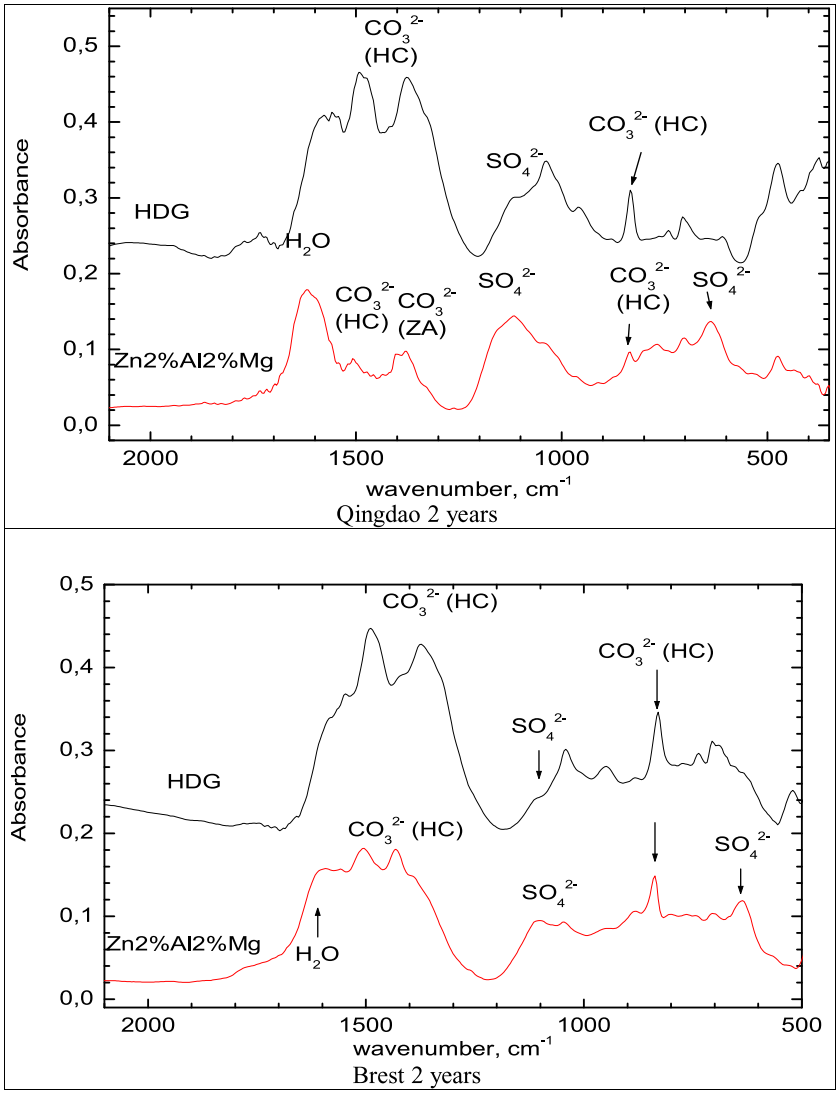

Fig. 12. FT-IRRAS spectra of HDG and Zn2%Al2%Mg coated steel exposed 2 years in Brest and Qingdao.

Table 5
Possible corrosion products, their chemical formula and abbreviations.

Name	Chemical formula	Abbreviation
Hydrozincite	$Zn_5(OH)_6(CO_3)_2$	HC
Simonkolleite	$Zn_5(OH)_8Cl_2{\cdot}H_2O$	SC
Gordaite	$NaZn_4(SO_4)(OH)_6Cl{\cdot}6H_2O$	G
Zinc hydroxy sulfate	$Zn_4(OH)_6\ SO_4{\cdot}3H_2O$	ZS3
	$Zn_4(OH)_6\ SO_4{\cdot}5H_2O$	ZS5
Aluminium hydroxy sulfate	$Al_2(OH)_4(SO_4)\ {\cdot}7H_2O$*	AS
Zincite	ZnO	ZnO
Layrered double hydroxide	$M(II)_xM(III)_y(A)_m(OH)_n{\cdot}zH_2O$ $M(II) = Zn^{2+}, (Mg^{2+})$ $M(III) = Al^{3+}$ $A = CO_3^{2-}, Cl^-, SO_4 2$	LDH
	$Zn_2Al(OH)_6(CO_3)_{1/2}{\cdot}zH_2O$**	ZA

* or similar compounds.
** PDF Card No.: 00-048-1023 or similar compounds.

GD-OES data was also used to obtain information about changes in the Mg and Al content in the coating layer upon exposure. The ratio between the coating weight of Mg and Al in the exposed samples to the unexposed samples gives information about how much Mg and Al which has dissolved from the coating during corrosion. If Mg and Al are dissolved from the coating the ratio between the coating weights for the exposed samples and the unexposed samples will decrease. If the ratio is close to one Mg and Al are still in metallic form, or is bonded in insoluble corrosion products in the surface layer. As seen in Table 8 more Mg dissolved from the coatings after exposure while Al was retained in the corrosion products or present in the metallic form. This is consistent with the SEM-EDS measurements which indicate that Mg is depleted in the corrosion products and that the Al containing corrosion products have formed.

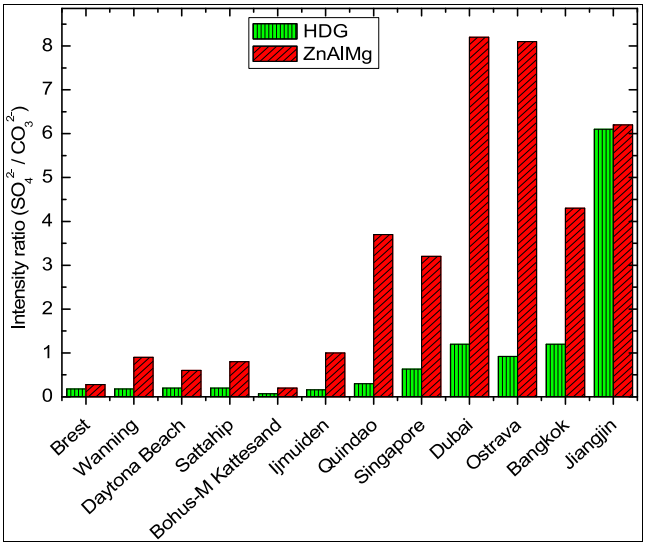

Fig. 13. Ratio of the intensities for the IR-peaks of sulfate (600 cm^{-1}) and carbonate.
(830 cm^{-1}) in the FT-IRRAS spectra for Zn2%Al2%Mg coated steel and HDG after 2 years exposure at different exposure sites world-wide. For HDG material exposed at Wanning was the transmission spectra of corrosion products used in the calculation.

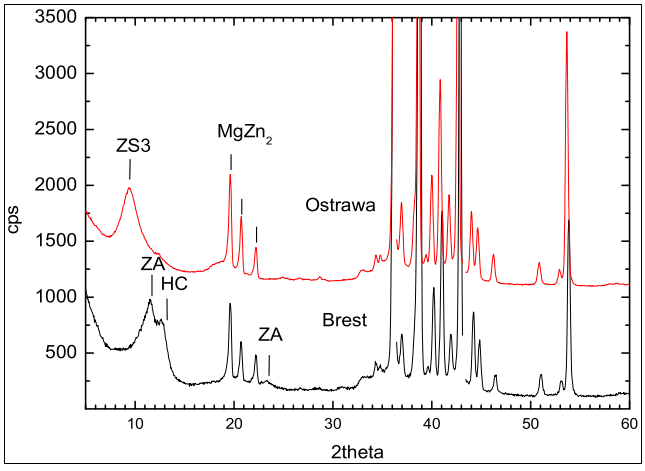

Fig. 14. X- ray diffractograms of Zn2%Al2%Mg coated steel after 2 years exposure in Brest (France) and.

4. Discussion

The atmospheric corrosion of the ZnAlMg coated steel results in localized corrosion attacks preferably at the eutectic phases of the alloy. The coating was penetrated to the steel surface already after 6 months of exposure with the formation of sulphate and chloride containing (at the marine test sites) corrosion products in the corrosion pits. The aluminum content in the corrosion products in the pits is enhanced while the magnesium is depleted from the corrosion products. The sulphate and chloride containing corrosion products are present largely in the pits while carbonate containing corrosion products are accumulated in the outer part of the coating. The analysis performed could not unambiguously identify all phases present in the corrosion products on the ZnAlMg coated steel but the results suggest that the corrosion products in the pits contain sulphate and chloride compounds with a high Al content. This could be zinc and aluminium hydroxyl sulphates or / and zinc/ aluminium sulphate and chloride based layered double hydroxides, $Zn_xAl_y(A)_m(OH)_n{\cdot}zH_2O$, where A is Cl^- or SO_4^{2-}. Zinc hydroxy carbonate is formed in much larger amounts mainly at the pure marine test sites, together with carbonate containing layered double hydroxide. However, in general the amount of carbonate containing corrosion products is smaller for the ZnAlMg coated steel compared to HDG. For industrial / urban exposure sites in which the SO_2 concentration is high, such as Jiangjin, transformation of carbonate containing products to sulphates might occur and carbonate compounds are found in low relative amounts.

No corrosion products associated with magnesium were identified and the depletion of magnesium from the corrosion products as indicated by the SEM-EDS and GD-OES measurements, is probably taking place largely during the initial stages of the corrosion with the formation of magnesium corrosion products which are dissolved and washed away from the ZnAlMg surfaces. It is possible that the magnesium play a role during the initial stages of the corrosion [11,12,14] were it can promote the formation of sulphate and chloride containing corrosion products and suppress the formation of ZnO [11], which could decrease the initial corrosion rate of the ZnAlMg coated steel. This effect could be explained by a reduction of the surface alkalinity by the formation of $Mg(OH)_2$ [11,14], which inhibit the cathodic oxygen reduction and the formation of zinc oxide, but promotes the formation of zinc hydroxy chloride and sulphate. The SEM-EDS maps and GD-OES measurements indicates that Mg is depleted from the corroded areas and as the magnesium become less accessible with longer exposure times, this effect will be less important with time. However, aluminium ions also precipitate readily as corrosion products and the results indicates that aluminium was retained in the corrosion pits, probably as sulphate containing corrosion products.

During exposure the corrosion attacks propagate in the eutectic phases and localized corrosion attacks are formed in the coating that are filled with corrosion products. As the eutectic regions are consumed zinc rich dendrites close to the coating / atmosphere interphase remains largely unaffected. A this stage, the cathodic reaction probably takes

Table 6
Possible phases in the corrosion products on HDG coated steel and Zn2%Al2% Mg coated by x-ray diffraction after 2 years exposure at world-wide exposure sites.

Exposure site	HDG [from ref. [8]]	ZnAlMg
Brest	HC, SC, G, ZS3, ZS5, Z	HC, ZA, ZS3, (SC)
Wanning	HC, SC, Z, G, ZS3	HC,ZA, ZS3, (SC)
Daytona Beach	HC, SC, ZS5, G	HC, ZA, ZS3, (SC)
Sattahip	ZS5, HC, SC	HC, ZS3
Bohus-Malmön, Kattesand	HC, SC, ZS5, G	HC, ZA, ZS3
Bohus-Malmön, Kvarnvik	HC, SC, ZS5, G	HC, ZA, ZS3
Ijmiuden	HC, SC, ZS4, G	ZA, ZS3 (HC), (SC)
Qingdao	HC, ZS, Z	ZS3, ZA
Singapore	ZS3, ZS5, HC, G	ZS3, ZA
Dubai	G, ZS5, HC, SC	ZS3, ZA
Cadiz	G, SC, ZS5, HC	ZS3, ZA
Ostrawa	ZS5, ZS3, HC	ZS3, (ZA)
Bangkok	ZS5, HC	ZS3, (ZA)
Jiangjin	ZS3	ZS3, (ZA)

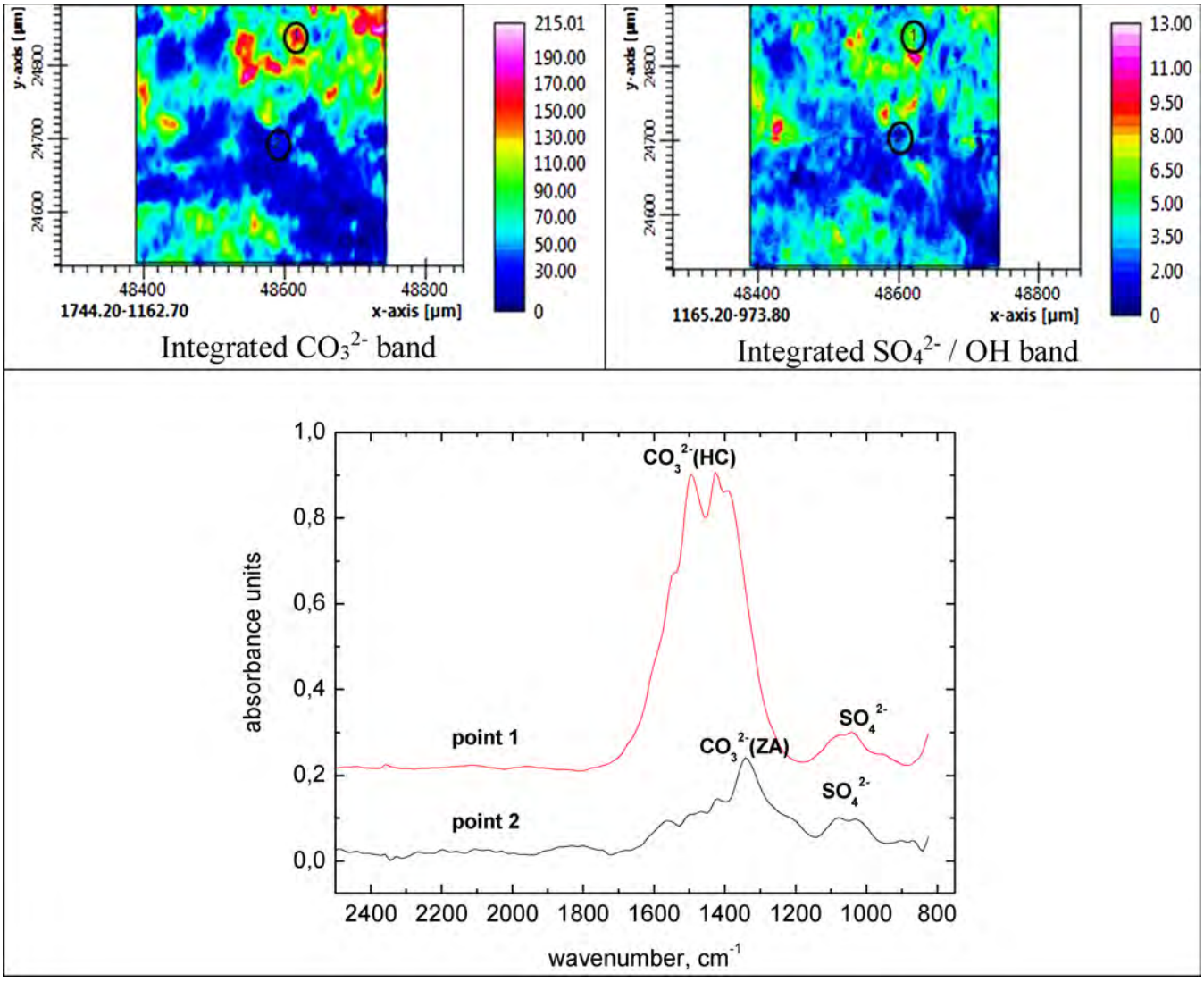

Fig. 15. FTIR-images of the integrated carbonate and sulphate bands for Zn2%Al2%Mg coated steel after 2 years exposure in Brest (France). FTIR reflection spectra in selected areas.

place on the Zn rich phases on the outer parts of the coating which is in closer contact with the atmosphere, and with access to oxygen and carbon dioxide. The corrosion pits are filled with corrosion products which restrict the transport of oxygen, as well as carbon dioxide to the interior part of the corrosion pits. Therefore it is likely that the oxygen reduction reaction takes place in the outer parts of the electrolyte covered coating. This increase the local pH at these parts which lead to the formation of zinc hydroxy carbonate and carbonate containing layered double hydroxides, such as $Zn_2Al(OH)_6(CO_3)_{1/2} \cdot zH_2O$ or similar. The Al could be supplied by the dissolution of the eutectics but also of aluminium containing corrosion products due to the more alkaline conditions at the cathodic areas. A schematic description of the propagation of the corrosion on ZnAlMg coated steel in marine and marine / industrial exposure sites is shown in Fig. 18.

It should be remembered that the corrosion of the HDG coated steel is localized as well, as seen in the previous investigation [8], with the formation of corrosion pits which penetrate the zinc coating after 6 months exposure time. In the marine sites, the chloride and sulphate containing corrosion products are accumulated in the pits and zinc hydroxy carbonate formed closer to the coating / atmosphere interface. Larger amount of zinc hydroxy carbonate is formed at the marine and marine / urban / industrial test sites. The overall corrosion mechanism is largely similar for HDG and ZnAlMg coated steel with the localized types of corrosion attack on both types of coatings. During the propagation of the corrosion anions such as sulphate and chloride are accumulated in the corrosion pits as a result of the formation of a local corrosion cell with a separation of the anodic reactions in the bottom of the corrosion pit while the cathodic reactions takes place in the outer parts, more close to the coating / atmosphere interface. The pits are filled with corrosion products which separate the anodic and cathodic areas of the corrosion cell. This also requires transport of ions through the corrosion product filled pits to maintain the electrochemical cell.

The mass loss for the ZnAlMg coated steel is smaller compared to HDG for all types of exposure sites, with a ratio of the mass loss for HDG

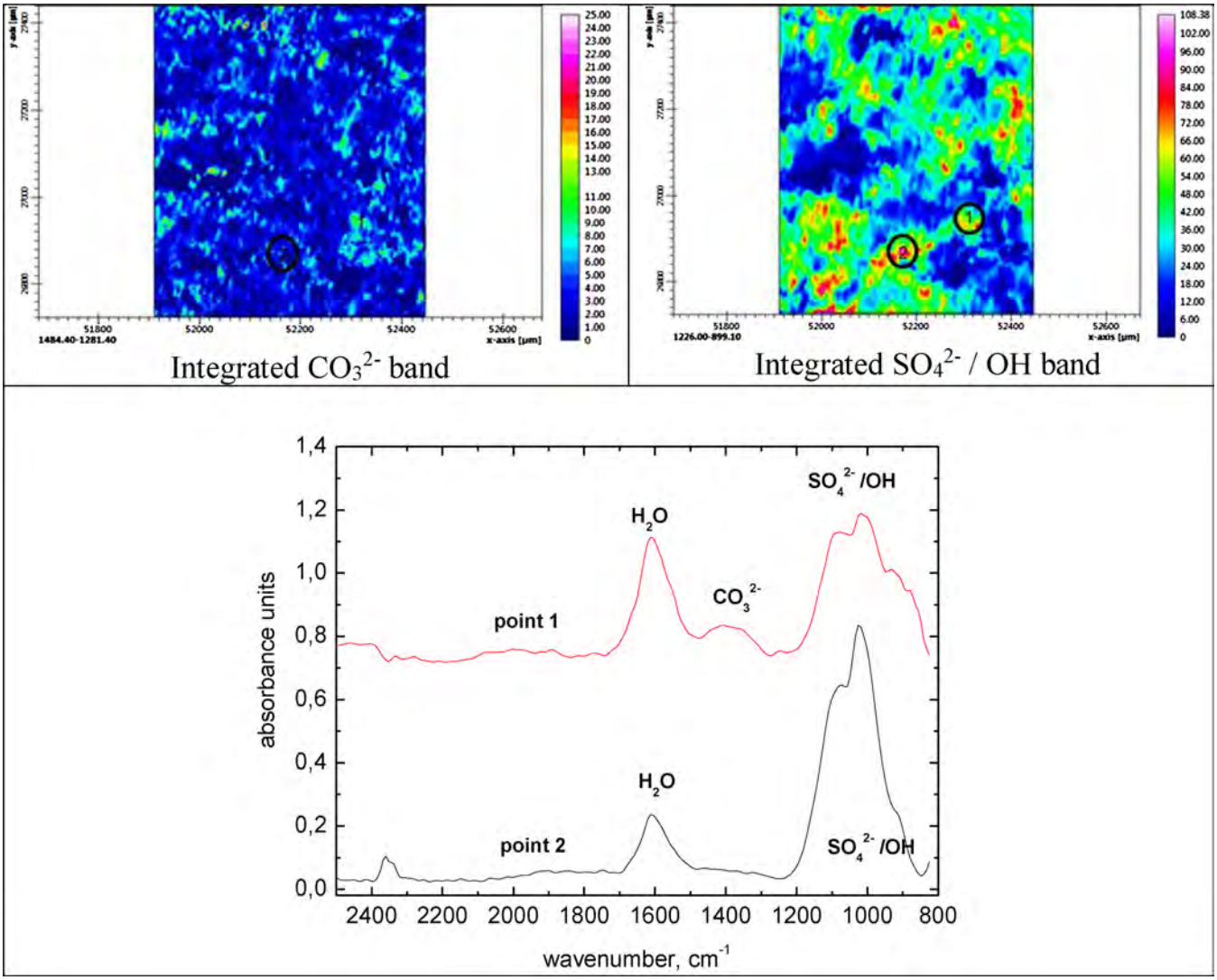

Fig. 16. FTIR-images of the integrated carbonate and sulphate bands for Zn2%Al2%Mg coated steel after 2 years exposure in Jiangjin (China). FTIR reflection spectra in selected areas.

vs ZnAlMg coated of 2–3 after 2 years exposure. The sulfate to carbonate ratio was also higher for the ZnAlMg coated steel implying that the formation of carbonate containing corrosion products, such as zinc hydroxy carbonate, is smaller compared to HDG. A substantial difference between HDG and ZnAlMg coated steel is the selective attack on the eutectic phases in the latter alloyed coating. The presence of Al and Mg is probably linked to the reduced formation of carbonate containing corrosion products for the ZnAlMg coated steel, and probably this is related to the cathodic processes which occur on the outer parts of the coating during the propagation of the corrosion. Aluminium and magnesium ions can form corrosion products which inhibit the oxygen reduction reaction that occurs at the coating surface. As suggested in a previous work [8], the zinc hydroxy carbonate which is formed on zinc has poor barrier properties and oxygen can be transported to the oxide covered surface where the cathodic reaction can take place. By the formation of other products in the outer parts of the coating, such as $Zn_xAl_y(A)_m(OH)_n{\cdot}zH_2O$, the efficiency of oxygen reduction can be reduced on the ZnAlMg coated steel and the corrosion rate reduced in comparison with HDG.

5. Conclusions

A wide world Atmospheric exposure of HDG and Zn2%Al2%Mg coated steel has been conducted on world-wide sites in Europe, East Asia and USA. The mass loss, the localization of corrosion attacks and the composition of the corrosion products were studied after 0.5, 1 and 2 years exposure. From the results of this investigation the following main conclusions can be drawn:

- The measured mass loss of Zn2%Al2%Mg coated steel was lower than that of HDG for all exposure sites and independently on climatic conditions. The ratio the mass loss after 4 years between HDG and Zn2%Al2%Mg coated steel was quite constant at most sites with a mean value at 2.2

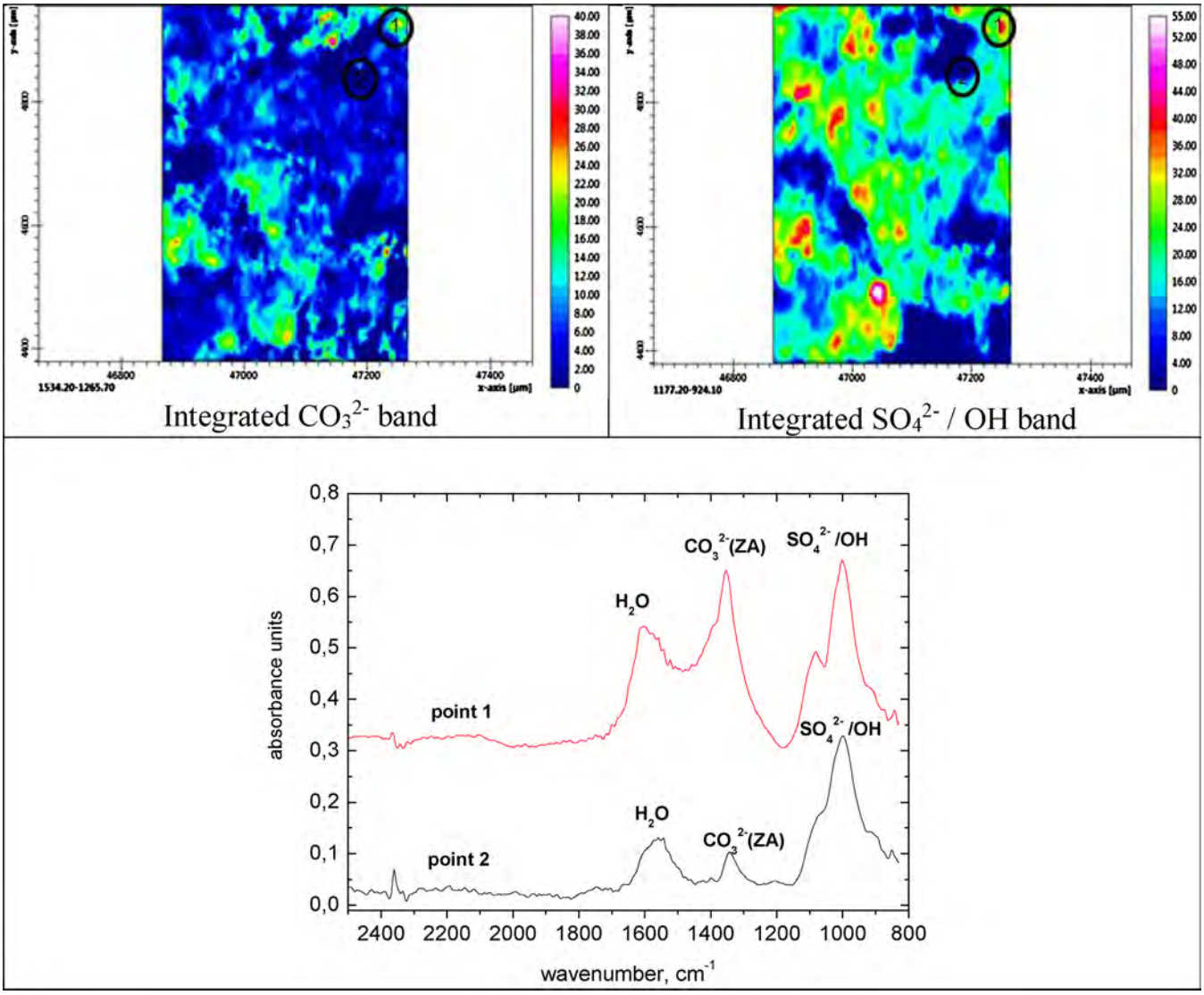

Fig. 17. FTIR-images of the integrated carbonate and sulphate bands for Zn2%Al2%Mg coated steel after 2 years exposure in Qingdao (China). FTIR reflection spectra in selected areas.

Table 7
Ratio of coating weights for Sulphur and Carbon after 2 years exposure on the outer parts of the coating (0–4 µm) and through the entire Zn2%Al2%Mg or HDG coating.

	Coating	Ratio (S/C) (0–4 µm)	Ratio (S/C) (whole coating
Qingdao	ZnAlMg	1,40	2,36
Jiangjin	ZnAlMg	1,58	2,91
Brest	ZnAlMg	0,65	0,95
Brest	HDG	0,27	0,38
Ostrawa	HDG	0,79	0,85

Table 8
Ratio of coating weights of magnesium and aluminium for exposed and unexposed samples of Zn2%Al2%Mg coated steel.

	Ratio($Mg_{exposed}$/ $Mg_{unexposed}$)	Ratio($Al_{exposed}$/ $Al_{unexposed}$)
Brest	0.78	0.84
Jiangjin	0.93	0.95
Qingdao	0.76	0.99

- The corrosion attack on the Zn2%Al2%Mg coated steel was localized and occurred preferentially in the eutectic phases of the coating, while the zinc rich phases remained largely unattacked. For marine and marine / industrial / urban sites sulphate and chloride containing corrosion products were formed in the corrosion pits while carbonate containing corrosion product, such as zinc hydroxy carbonate and carbonate containing layered doubly hydroxides (LDH), were formed on the outer parts of the coating.
- The formation of corrosion products on the Zn2%Al2%Mg coated steel and HDG was related to the formation of local corrosion cells at the surface and the concomitant differences in the local chemistry of the surfaces.

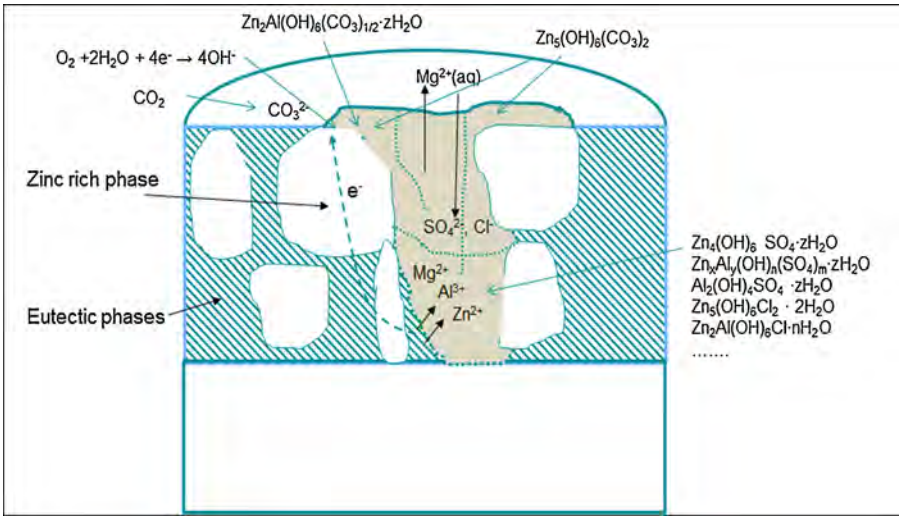

Fig. 18. Schematic model of the propagation of atmospheric corrosion of for Zn2%Al2%Mg coated steel in marine, marine/urban and marine/industrial atmosphere.

- The type of corrosion products on Zn2%Al2%Mg coated steel HDG differ depending on the type of environment (e.g. marine, marine industrial and industrial) with less formation of zinc hydroxy carbonate and relatively more sulphate containing corrosion products in marine industrial and industrial sites compared to “pure” marine sites. The ratio of sulphate to carbonate was generally higher for Zn2%Al2%Mg coated steel and may be linked to the corrosion rate of the coating with less formation of zinc hydroxyl carbonate on the latter material.

Acknowledgements

We acknowledge Oskar Karlsson for performing the SEM-EDS investigations and Fredrik Lindberg for help with the XRD-measurements.

References

[1] T. Tsujimura, A. Komatsu, A. Andoh, Brussels, BelgiumProc. Galvatech’ 01, International Conference on Zinc and Zinc Alloy Coated Steel2001, Proc. Galvatech’ 01, International Conference on Zinc and Zinc Alloy Coated Steel (2001) 145–152.
[2] T. Koll, K. Ullrich, J. Faderl, J. Hagler, A. Spalek, IL, United StatesProc. Galvatech’ 04, 6th International Conference on Zinc and Zinc Alloy Coated Steel Chicago2004, Proc. Galvatech’ 04, 6th International Conference on Zinc and Zinc Alloy Coated Steel Chicago (2004).
[3] S. Schürz, G.H. Luckeneder, K. Preis, T. Haunschmied, G. Mori, A.C. Kneissl, Corros. Sci. 51 (2009) 2355–2363.
[4] S. Schürz, G.H. Luckeneder, M. Fleischanderl, P. Mack, H. Gsaller, A.C. Kneissl, G. Mori, Corros. Sci. 52 (2010) 3271–3279.
[5] N.C. Hosking, M.A. Strom, P.H. Shipway, C.D. Rudd, Corros. Sci. 49 (2007) 3669–3695.
[6] T. Prosek, N. Larche, M. Vlot, F. Goodwin, D. Thierry, Mater. Corros. 60 (2010) 412–420.
[7] D. Thierry, T. Prosek, N. Le Bozec, E. Diller, Genova, ItalyProc. Galvatech. 2011, 8th International Conference on Zinc and Zinc Alloy Coated Steel2011, Proc. Galvatech. 2011, 8th International Conference on Zinc and Zinc Alloy Coated Steel (2011).
[8] D. Persson, D. Thierry, O. Karlsson, Corros. Sci. 126 (2017) 152–165.
[9] I.S. Cole, W.D. Ganther, S.A. Furman, T.H. Muster, A.K. Neufeld, Corros. Sci. 52 (2010) 848–858.
[10] Z. Cui, X. Li, K. Xiao, C. Dong, Z. Liu, L. Wang, Corrosion 70 (2014) 731–748.
[11] E. Diler, B. Rouvellou, S. Rioual, B. Lescop, G. Nguyen Vien, D. Thierry, Corros. Sci. 87 (2014) 111–117.
[12] M. Salgueiro Azevedo, C. Allély, K. Ogle, P. Volovitch, Corros. Sci. 90 (2015) 472–481.
[13] A. Tomandl, E. Labrenz, Mater. Corros. 67 (2016) 1286–1293.
[14] P. Volovitch, T.N. Vu, C. Allély, A. Abdel, A. Abdel Aal, K. Ogle, Corros. Sci. 53 (2011) 2437–2445.
[15] N. LeBozec, D. Thierry, A. Peltola, L. Luxem, G. Luckeneder, G. Marchiaro, M. Rohwerder, Corrosion performance of ZnMgAl coated steel in accelerated corrosion tests used in the automotive industry and field exposures, Mater. Corros. 64 (2013) 969–978.
[16] T. Prosek, N. Larché, M. Vlot, F. Goodwin, D. Thierry, Corrosion performance of ZnAlMg coatings in open and confined zones in conditions simulating automotive applications, Mater. Corros. 60 (2010) 412–420.
[17] D. Persson, D. Thierry, N. Lebozec, T. Prosek, Corros. Sci. 72 (2013) 54–63.